Air Gap Effect on Antenna Characteristics of Slitline and Stripline Dipoles on an Extended Hemispherical Lens Substrate

Truong Khang Nguyen [1,2] and Huy Hung Tran [1,2,*]

[1] Division of Computational Physics, Institute for Computational Science,
Ton Duc Thang University, Ho Chi Minh City, Vietnam

[2] Faculty of Electrical and Electronics Engineering, Ton Duc Thang University, Ho Chi Minh City, Vietnam
nguyentruongkhang@tdtu.edu.vn, *tranhuyhung@tdtu.edu.vn

Abstract ─ This paper presents the effect of an air gap introduced between a planar feed and an extended hemispherical lens on the antenna's impedance, current distribution and radiation characteristics. Two selected planar feeds for study are slitline dipole and stripline dipole. The results showed that as a small gap is introduced, the input impedance of the slitline dipole was almost remained unchanged while that of the stripline dipole was changed remarkably. More importantly, the boresight gain and radiation efficiency of the slitline dipole was improved whereas those of the stripline dipole were degraded with the presence of this air gap. An overall performance comparison for these two designs will be detailed in the paper. This study provides useful guidelines of choosing the proper feed for THz integrated lens antenna applications, especially for indoor THz communication applications such as wireless local area networks and wireless personal area networks in the 300 GHz band.

Index Terms ─ Air gap, extended hemispherical lens, leaky lens, slitline dipole, stripline dipole.

I. INTRODUCTION

Slot or dipoles feed used in combination with elliptical dielectric lens have been studied intensely for decades in harmonic or pulse systems [1-7]. Such integrated antenna is one of the key parts in high frequency sensing systems such as terahertz-time domain spectroscopy (THz-TDS), i.e., sub-mm waves, that couples the incoming radiation into the receiver [8, 9]. The reason for their important role is that antennas operating in the presence of dielectric lens have significantly improved the front to back ratios and increased the Gaussian coupling efficiency (Gaussicity), while eliminating substrate modes. In addition, as the antenna is printed directly on the top of the substrate lens, its fabrication offers greater dimensional accuracy and durability, and reduced cost than waveguide or waffled structures [10, 11]. More importantly, a planar integrated lens antenna with an optimum lens substrate and antenna structure plays a critical role in optimizing output power design for particular applications [12-16]. In other words, by choosing the proper feed and optimizing the lens substrate, the impedance and radiation characteristics of a planar integrated lens antenna can be significantly improved, which is essential to the output power of a system.

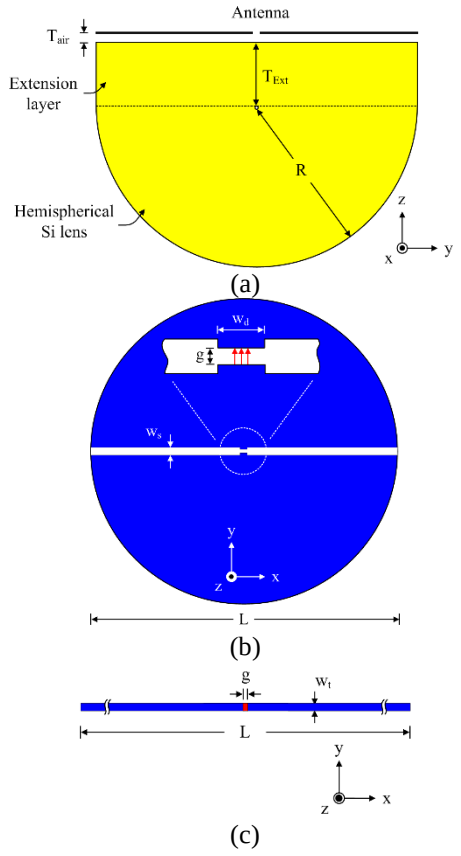

Fig. 1. Geometry of the antenna with an introduced air gap: (a) side view, (b) top view of the slitline dipole, and (c) top view of the stripline dipole.

Submitted On: May 15, 2018
Accepted On: September 10, 2018

The effect of an air gap between a leaky-wave slit and a high-permittivity substrate, i.e., semi-infinite or lens, has been studied theoretically and demonstrated experimentally [17-22]. It was found that a very small gap separation distance in terms of wavelength improved coupling efficiency and changed the propagation characteristics along the slit while simultaneously maintaining the directive radiation characteristics. However, a detailed study about this air gap effect on the overall performance of the integrated lens antenna with different planar feeds has received somewhat less attention, particularly at high frequency.

In this paper, we study in detail about this air gap effect on the input impedance, current distribution and radiation characteristics of integrated dielectric lens antennas with different planar feed, that are slitline dipole, i.e., slotline with open ends, and stripline dipole. Numerical results showed that the input impedance of the slitline dipole remained almost unchanged with the presence of such air gap while that of the stripline dipole have changed significantly. The radiation characteristic of the slitline dipole was improved for introducing such small air gap whereas that of the stripline dipole was somehow degraded. These observations provide guidelines in choosing a proper planar feed and an optimum air gap in such leaky lens design for particular application purposes.

II. ANTENNA GEOMETRIES

Figure 1 (a) shows the prototype of an antenna on an extended hemispherical lens fully made of silicon (lossless, $\varepsilon_r = 11.9$). The extension layer and radius of the lens are denoted by T_{Ext} and R, respectively. The thickness of the extension layer and the radius of the Si lens are 1.8 mm and 5.0 mm, respectively, which corresponding to a ratio $T_{Ext}/R = 0.36$ for the best possible gain performance [12]. An air gap is introduced between the feed and the leaky lens and is designated as T_{air}. Figures 1 (b) and (c) shows the geometries of the two selected planar feeds that are slitline dipole and stripline dipole. The metal layer for the ground of the slitline dipole and for the stripline dipole had a conductivity of 1.6×10^7 S/m and a thickness of 0.35 mm. The widths of the slitline dipole and the stripline dipole are denoted as w_s and w_t, respectively. Both the slitline dipole and the stripline dipole have a same total length of L which equals to the diameter of the leaky lens. A short dipole was modeled at the slitline center to drive a current source through the slit. The feeding gap for both the slitline dipole and the stripline dipole are designated as g. Design parameters are fixed throughout the study as follows: $w_s = w_t = w_d = 10$ µm, $g = 5$ µm, and $L = 10$ mm. The full-wave simulator Microwave Studio by CST based on the finite-integration time-domain (FIT) technique was used to investigate the antenna characteristics [23]. In the simulation, the antenna was excited by the discrete port feeding with an "S-parameter" source, i.e., a current source with the reference impedance of 50 Ω. This model allows excitation of the entire gap with the S-parameter model to compute the S- and Z-parameters. For the radiation characteristics, principally open boundaries, but with some added space boundaries, were used to accurately calculate the antenna radiation patterns. Accordingly, all the gains and radiation efficiencies shown in the following results are deduced from the radiation patterns of the antenna at the frequencies of interest.

III. ANTENNA CHARACTERISTICS

A. Impedance characteristics

We first studied the air gap effect on the impedance characteristics of the slitline and stripline dipoles. Then, we studied the behavior of impedance characteristics with respect to frequency variation. Figure 2 shows the real and imaginary parts of input impedance with respect to air gap range of 0~50 µm with an increment of 5 µm at the fixed frequency of 300 GHz. Input resistance of slitline dipole increased linearly from 48 Ω to 50 Ω with an increase in air gap from 0~10 µm. From 10~40 µm, it showed a smooth increment of 10 Ω from 50 Ω to 60 Ω. After 40 µm, it became stable and reached a saturation value of 62.5 Ω, as illustrated in Fig. 2 (a). However, the stripline dipole showed completely different behavior, input resistance significantly increased from 75 Ω to 225 Ω with an increase in air gap from 0~20 µm. After 20 µm, input resistance reached the saturation value of 275 Ω. The imaginary part of the input impedance of slitline dipole and stripline dipole showed the inductive and capacitive behavior, respectively, as illustrated in Fig. 2 (b). Input reactance of slitline dipole slightly increased from 12.5 Ω to 25 Ω with an increase in air gap from 0~5 µm. After 5 µm, it reached the saturation value of 30 Ω. Input reactance of stripline dipole decreased from 120 Ω to 100 Ω with an increase in air gap from 0~5 µm. From 5~40 µm, input reactance showed an increment of 70 Ω, so the value varied from 100 Ω to 170 Ω. After 40 µm, it reached the saturation value of 170 Ω. From simulation results, we observed that the input impedance of the stripline dipole had a higher value as compared to the slitline dipole. When, we introduced the air gap between the feed and leaky lens, in case of stripline dipole effective permittivity seen by dipole towards the substrate side reduced, as a result, impedance increased with an increase in the air gap. However, in case of slitline dipole due to the presence of long ground plane, the effective permittivity seen by dipole towards substrate side remained same, as a result, the impedance characteristics remained stable and smooth with or without the air gap. This is the reason that the input impedance of slitline dipole remains the same, while for stripline dipole it significantly increased with air gap variation. From these results, it can be concluded that the slitline dipole supported wideband impedance bandwidth and its input impedance was very slightly

affected by the presence of the air gap. In contrast, the stripline dipole showed a possibility in increasing its input impedance by introducing the air gap and thus would be appropriate for a design with a high input impedance requirement.

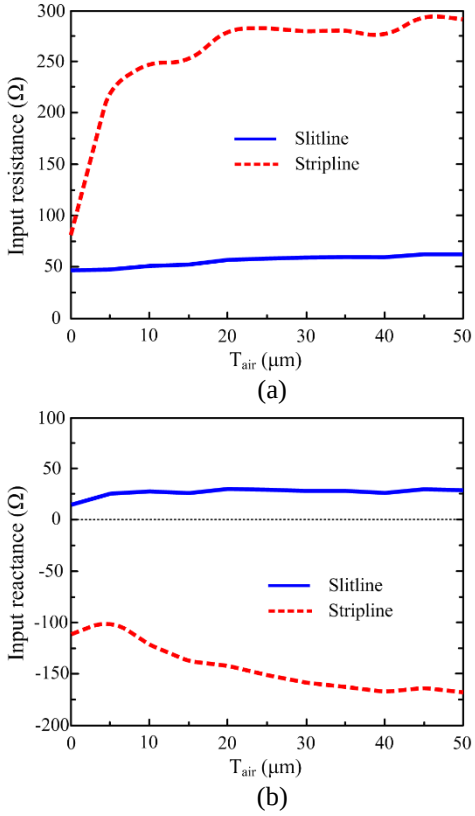

Fig. 2. (a) Input resistance and (b) input reactance (at 300 GHz) as a function of the air gap, T_{air}, in a comparison between slitline and stripline dipoles.

Figure 3 showed the impedance behavior of slitline and stripline dipoles over a broad frequency range of 100~500 GHz at three selected air gaps of 0 μm, 5 μm, and 10 μm. Generally, the input resistance of the slitline dipole slightly increased whereas that of the stripline dipole significantly decreased with the increase in frequency from 100 GHz to 500 GHz. The input resistance of the slitline dipole without air gap (T_{air} = 0 μm) remained stable around 25 Ω and exhibited a slight average increment of 5Ω as we introduced the air gap of 5 μm. However, as we further increased the air gap from 5 μm to 10 μm, the input resistance remained the same as that of the 5 μm case. In contrast, the input resistance of the stripline dipole showed a remarkable variation, i.e., gradually decreased with an amplitude of about 75 Ω, as the frequency increased from 100 GHz to 500 GHz. It can be seen that the presence of the air gap maintained the impedance trend but significantly increased the impedance level of the stripline dipole, observed in Fig. 3 (a) as T_{air} varied from 0 μm to 5 μm. However, as the air gap was further increased from 5 μm to 10 μm, the impedance level only showed a slight increase.

The input impedance behavior of the slitline and stripline dipoles in a function of frequency is illustrated in Fig. 3 (b). The input reactance of the slitline dipole was stable and showed small variation within the frequency of interest either for introducing a small air gap of 5 μm or further increasing this air gap from 5 μm to 10 μm which is similar with its input resistance behavior. However, the input reactance of the stripline dipole exhibited differently with its input resistance. The input reactance of the stripline dipole was gradually decreased with the increase of frequency for the case of without air gap T_{air} = 0 μm. However, as a small air gap introduced, its input reactance was gradually increased with the increase of the frequency, as seen for T_{air} = 5 μm and T_{air} = 10 μm. From these results, we can conclude that the air gap has significantly influenced the impedance profile of the stripline dipole but only has slightly impacted the impedance profile of the slitline dipole. In addition, the impact level was remarkable for a state change from without (T_{air} = 0 μm) to with (T_{air} = 5 μm) and was insignificant for further increasing this air gap.

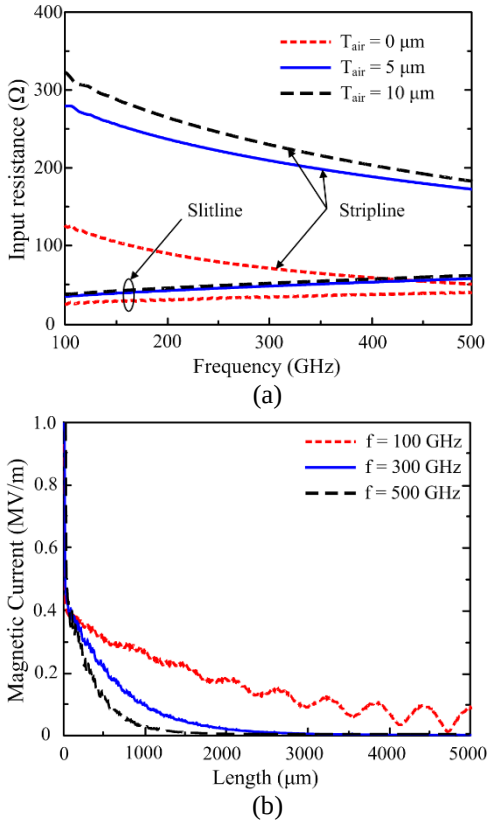

Fig. 3. (a) Input resistance and (b) input reactance as a function of frequency in a comparison between the slitline and stripline dipoles for different air gaps.

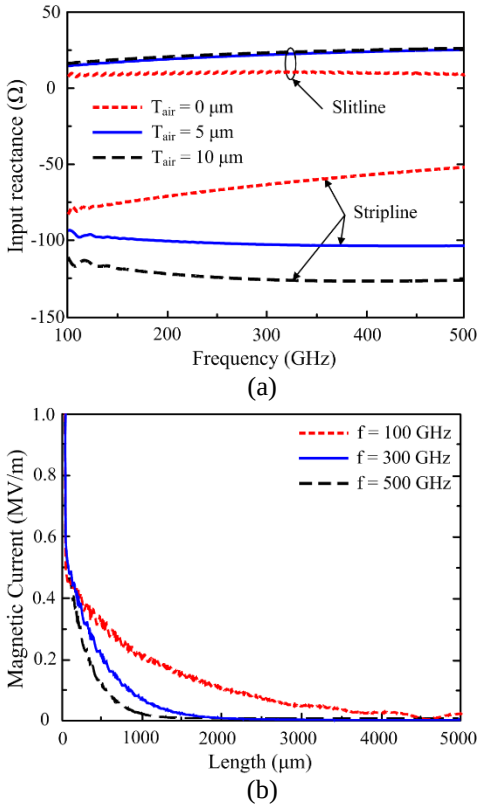

Fig. 4. Magnetic current distribution along the slitline dipole at different frequencies: (a) without air gap (T_{air} = 0 μm), and (b) with air gap (T_{air} = 5μm).

B. Current distribution

Figures 4 and 5 show the distributions of surface current over half of the length of the slitline and stripline dipoles, respectively. We considered the two cases of the air gap, i.e., without air gap (T_{air} = 0 μm) and with air gap (T_{air} = 5 μm), at three different selected frequency values of 100 GHz, 300 GHz, and 500 GHz. A general trend was observed in both stripline and slitline dipoles that the current attenuation increased with increasing the frequency [17]. At a very low frequency of 100 GHz, both the stripline and slitline dipoles exhibited a surface current with standing-wave behavior characterized by the reflection at their terminations. At higher frequencies of 300 GHz and 500 GHz, the surface currents were attenuated more rapidly and consequently left behind no current to be reflected back. From the magnetic current of the slitline dipole illustrated in Fig. 4, we observed that the current attenuated more rapidly for the air gap case in comparison with the without air gap case. In addition, the current distribution in the feeding area, i.e., near the 0-value of length, of the slitline dipole with the air gap was higher than that of the slitline dipole without the air gap. Figure 5 also presented that the current along the stripline dipole attenuated more rapidly for the air gap case in comparison with the without air gap case. However, in contrast with the slitline dipole, the current distribution in the feeding area of the stripline dipole with the air gap was lower than that of the stripline dipole without the air gap. These results indicate that the presence of the air gap yielded a positive effect of increasing the current distribution localized at the feeding area of the slitline dipole whereas exhibiting a negative effect of decreasing the current distribution localized at the feeding area of the stripline dipole.

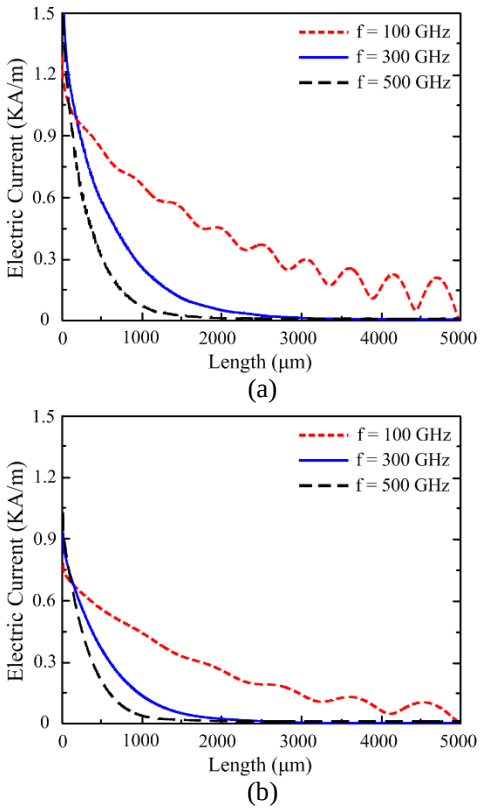

Fig. 5. Electric current distribution along the stripline dipole at different frequencies: (a) without air gap (T_{air} = 0 μm), and (b) with air gap (T_{air} = 5μm).

C. Radiation characteristics

To study the radiation characteristics, we first investigated the boresight gain (at θ = 180°) and radiation efficiency of the stripline and slitline dipoles with respect to air gap at a fixed frequency of 300 GHz, as illustrated in Figs. 6 (a) and 6 (b), respectively. The boresight gain of slitline dipole exponentially increased from 21 dBi to 25 dBi as the air gap increased from 0 μm to 5 μm, then slightly decreased from 25 dBi to 23 dBi as the air gap increased from 5 μm to 20 μm, and then linearly decreased from 23 dBi to 19 dBi as the air gap increased from 20 μm to 50 μm. The boresight gain of the stripline dipole, however, gradually decreased with an increase of the air gap from 0 μm to 50 μm. These behaviors can be explained from the current distributions at the feeding

area of the slitline and stripline dipoles as observed in Figs. 4 and 5. The radiation efficiency of the slitline and stripline dipoles followed the similar trend like that of boresight gain up to 20 µm, but after 20 µm, they became stable with an increase in the air gap. The simulation results indicate that the small air gap has improved the radiation characteristics in term of boresight gain and radiation efficiency of the slitline dipole. The gain and radiation efficiency of the slitline dipole at this optimized air gap, i.e., 25 dBi and 82%, were slightly improved in comparison with the stripline dipole without the air gap, i.e., 24 dBi and 80%. In addition, the slitline dipole with the air gap (T_{air} = 5 µm) would be appropriate choice to select because of its large ground plane that allows the active devices to be easily integrated.

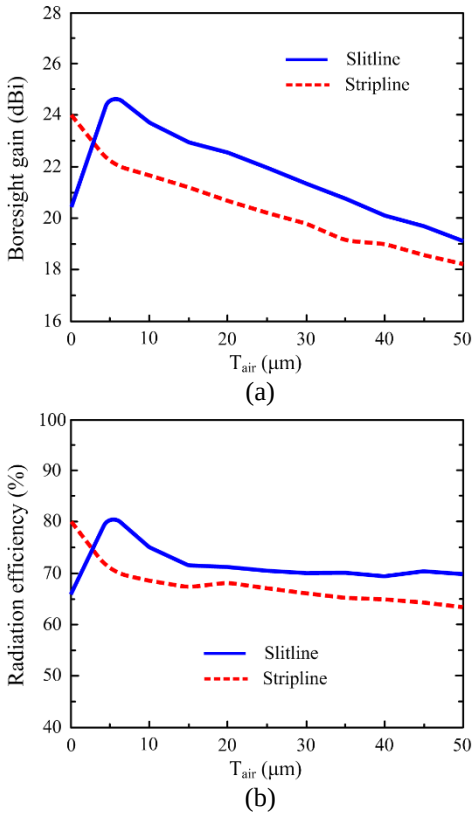

Fig. 6. (a) Boresight gain and (b) radiation efficiency at 300 GHz as a function of the air gap, T_{air}, in a comparison between slitline and stripline dipoles.

Secondly, we investigated the boresight gain (at θ = 180°) and radiation efficiency of slitline dipole and stripline dipole as a function of frequency, i.e., from 100 GHz to 500 GHz, with three selected air gap values of 0 µm, 5 µm, and 10 µm, as shown in Fig. 7 and Fig. 8, respectively. Generally, the boresight gain of slitline dipole and stripline dipole increased with increase in frequency. The boresight gain of the slitline dipole without air gap increased from 12.5 dBi to 23 dBi as frequency increased from 100 GHz to 500 GHz, however, it contained two peaks and one dip. The first and second peaks occurred at frequency values of 200 GHz and 415 GHz with the magnitudes of 22.5 dBi and 27 dBi, respectively. The dip occurred at 300 GHz with the magnitude of 20 dBi. When we introduced the air gap of 5 µm and 10 µm, the boresight gain became smooth and stable and in addition, linearly increased and reached a saturation at a frequency around 300 GHz. The boresight gain versus frequency of the stripline dipole behaved differently. The boresight gain of the stripline dipole had peaks and dips for all three cases of the air gap over the whole frequency range of interest. The introduced air gap did not modify the boresight gain profile of the stripline dipole as the slitline dipole did. The radiation efficiency of the slitline and stripline dipoles behaved similarly with the gain. The stripline dipole without air gap even presented its radiation efficiency with smaller variation than that of the slitline dipole within the frequency range of interest.

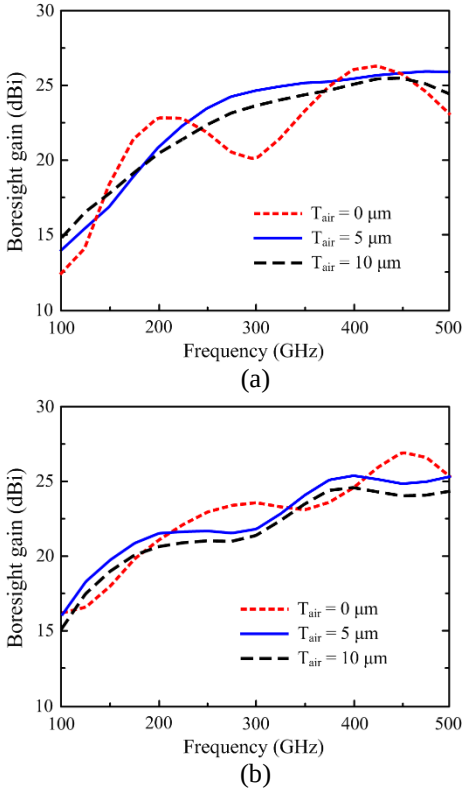

Fig. 7. Boresight gain versus frequency with respect to the air gap variation: (a) slitline dipole and (b) stripline dipole.

Lastly, we checked and compared the radiation patterns of the slitline dipole and stripline dipole at 300 GHz in *E*-plane and *H*-plane with two cases of air gap, i.e., without air gap (T_{air} = 0 µm) and with air gap (T_{air} = 5 µm), as shown in Fig. 9 and Fig. 10, respectively. From

Fig. 9, we observed that the radiation pattern of the slitline dipole with an air gap of 5 μm in both *E*- and *H*-planes had higher boresight gain than the case of without air gap. As introducing an air gap of 5 μm, the width of the main beam in the *E*-plane remained whereas that in the *H*-plane became broader because the side lobes merged together. From Fig. 10, we observed that the radiation pattern of stripline dipole without air gap in both *E*- and *H*-planes had higher boresight gain than the case of with air gap. In addition, the back radiations of stripline dipole also reduced both in number and magnitude with increase in the air gap, and beamwidths remained the same for both cases. These observed gain behaviors result from the changes of the relative refractive indices of the lower space, which determines the distribution of the radiation of the dipole [24]. While the relative refractive index was reduced by introducing the small air gap under the stripline dipole, that of the slitline dipole case was increased thanks to the resonant cavity effect [17]. It can be seen that the air gap of 10 μm, corresponding to $0.01\lambda_o$ at the frequency of 300 GHz, can be used to enhance the antenna gain, which relatively agrees with the experimental results of others [20, 25]. However, the air gap should be smaller and optimized carefully to maximize the gain enhancement of the antenna at the frequency range of interest.

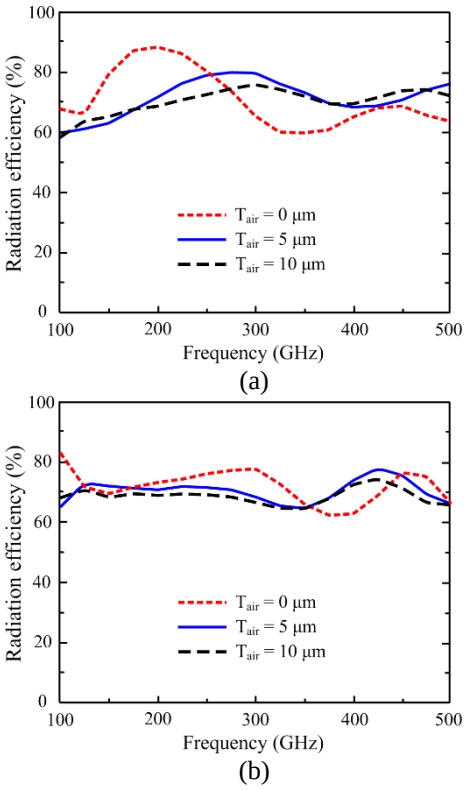

Fig. 8. Radiation efficiency versus frequency with respect to the air gap variation: (a) slitline dipole and (b) stripline dipole.

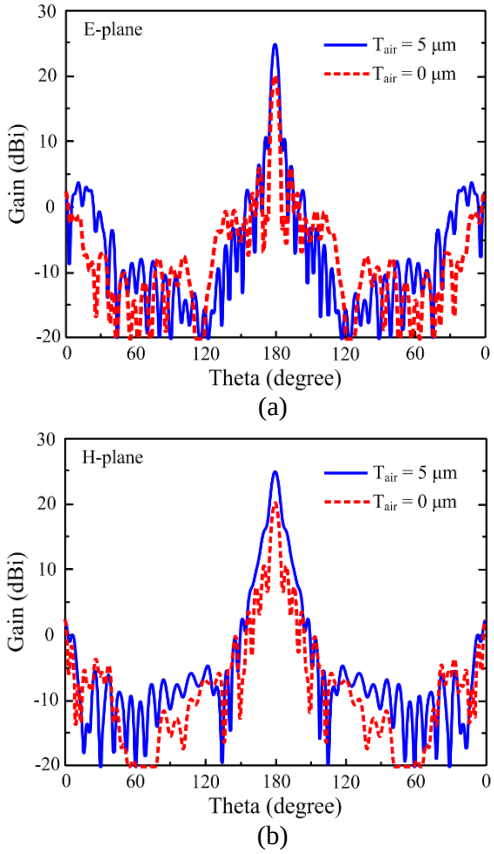

Fig. 9. Radiation patterns at 300 GHz of the slitline dipole with and without the air gap: (a) E-plane and (b) H-plane.

VI. CONCLUSION

A leaky-wave slitline dipole antenna and a traveling wave stripline dipole antenna designed on extended hemisphere Silicon lens were numerically evaluated by introducing the air gap between the lens and the antenna. The influence of the air gap on the antennas' impedance, current distribution and radiation characteristics is studied. The input impedance of stripline dipole showed a remarkable change with introducing a small air gap while it remained almost the same in case of the slitline dipole. The current distribution at the low frequency of the slitline dipole with the presence of the air gap was more stable and smooth than that of the stripline dipole. In the radiation characteristic consideration, the boresight gain and radiation efficiency of the slitline dipole with the presence of air gap was more likely improved while that of stripline it showed degradation. This study provides useful guidelines of choosing the proper feed for THz integrated lens antenna applications, especially for indoor THz communication applications such as wireless local area networks and wireless personal area networks in the 300 GHz band.

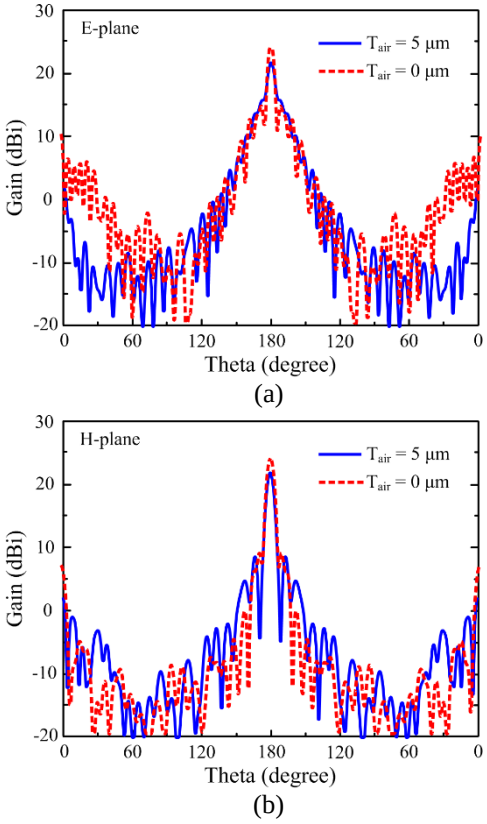

Fig. 10. Radiation patterns at 300 GHz of the stripline dipole with and without the air gap: (a) E-plane and (b) H-plane.

ACKNOWLEDGMENT

T. K. Nguyen would like to thank TWAS (16-184 RG/PHYS/AS_I-FR3240293349).

REFERENCES

[1] D. F. Filippovic, S. S. Gearhart, and G. M. Rebeiz, "Double slot on extended hemispherical and elliptical silicon dielectric lenses," *IEEE Trans. Microw. Theory Techn.*, vol. 41, no. 10, pp. 1738-1749, Oct. 1993.

[2] A. Neto, D. Pasqualini, A. Toccafondi, and S. Maci, "Mutual coupling between slots under an elliptical dielectric lens," *IEEE Trans. Antenn. Propag.*, vol. 47, no. 10, pp. 647-650, Oct. 1999.

[3] M. J.M. van der Vorst, P. J. I. de Maagt, A. Neto, A. L. Reynolds, R. M. Heeres, W. Luinge, and M. H. A. J. Herben, "Effect of internal reflections on the radiation properties and input impedance of integrated lens antennas-comparison between theory and measurements," *IEEE Trans. Microw. Theory Techn.*, vol. 49, no. 6, pt. 1, pp. 1118-1125, June 2001.

[4] X. Wu, G. Eleftheriades, and T. E. van Deventer-Perkins, "Design and characterization of single and multiple beam MM-wave circularly polarized substrate lens antennas for wireless communications," *IEEE Trans. Microw. Theory Techn.*, vol. 49, no. 3, Mar. 2001.

[5] A. D. Semenov, H. Richter, H.-W. Hubers, B. Gunther, A. Smirnov, K. S. Il'in, M. Siegel, and J. P. Karamarkovic, "Terahertz performance of integrated lens antennas with a hot-electron bolometer," *IEEE Trans. Microw. Theory Techn.*, vol. 55, no. 2, pt. 1, pp. 239-247, Feb. 2007.

[6] A. V. Boriskin, G. Godi, R. Sauleau, and A. I. Nosich, "Small hemielliptic dielectric lens antenna analysis in 2-D: Boundary integral equations versus geometrical and physical optics," *IEEE Trans. Antennas Propag.*, vol. 56, no. 2, pp. 485-492, Feb. 2008.

[7] A. V. Boriskin, R. Sauleau, and A. I. Nosich, "Performance of hemielliptic dielectric lens antennas with optimal edge illumination," *IEEE Trans. Antenn Propag.*, vol. 57, no. 7, pp. 2193-2198, July 2009.

[8] G. Chattopadhyay, M. Alonso-delPino, N. Chahat, D. González-Ovejero, C. Lee, and T. Reck, "Terahertz antennas and feed," In: Boriskin A., Sauleau R. (eds), *Aperture Antennas for Millimeter and Sub-Millimeter Wave Applications. Signals and Communication Technology*, Springer, Cham, 2018.

[9] C. Caglayan, G. C. Trichopoulos, and K. Sertel, "Hybrid electromagnetic modeling of lens-integrated antennas for noncontact on-wafer characterization of THz devices and integrated circuits," *ACES Express Journal*, vol. 1, no. 2, pp. 72-75, 2016.

[10] H. Hashiguchi, K. Kondo, T. Baba, and H. Arai, "An optical leaky wave antenna by a waffled structure," *J. Lightwave Technol.*, vol. 35, no. 11, pp. 2273-2279, 2017.

[11] K. Konstantinidis, A. P. Feresidis, C. C. Constantinou, E. Hoare, M. Gashinova, M. J. Lancaster, and P. Gardner, "Low-THz dielectric lens antenna with integrated waveguide feed," *IEEE Trans. Terahertz Sci. Technol.*, vol. 7, no. 5, pp. 572-581, 2017.

[12] I. Woo, T. K. Nguyen, H. Han, H. Lim, and I. Park, "Four-leaf-clover-shaped antenna for a THz photomixer," *Opt. Express*, vol. 18, no. 18, 18532-18542, Aug. 2010.

[13] T. K. Nguyen, S. Kim, F. Rotermund, and I. Park, "Design of a wideband continuous-wave photomixer antenna for terahertz wireless communication systems," *J. Electromagn. Waves Appl.*, vol. 28, no. 8, pp. 976-988, Apr. 2014.

[14] T. K. Nguyen, F. Rotermund, and I. Park, "A traveling-wave stripline dipole antenna on a substrate lens at terahertz frequency," *Curr. Appl.*

Phys., vol. 14, pp. 998-1004, May 2014.

[15] T. K. Nguyen, S. Kim, and I. Park, "Impact of varying the DC bias stripline connection angle on terahertz coplanar stripline dipole antenna characteristics," *J. Electromagn. Waves Appl.*, vol. 27, no. 14, pp. 1725-1734, 2013.

[16] A. Neto, "UWB, non-dispersive radiation from the planarly fed leaky lens antenna–Part 1 theory and design," *IEEE Trans. Antenn. Propag.*, vol. 58, no. 7, pp. 2238-2247, 2010.

[17] N. Llombart, G. Chattopadhyay, A. Skalare, and I. Mehdi, "Novel terahertz antenna based on a silicon lens fed by a leaky wave enhanced waveguide," *IEEE Trans. Antenn. Propag.*, vol. 59, no. 6, pp. 2160-2168, 2011.

[18] N. Llombart and A. Neto, "THz time-domain sensing: the antenna dispersion problem and a possible solution," *IEEE Trans. Terahertz Sci. Technol.*, vol. 2, no. 4, pp. 416-423, 2012.

[19] D. Cavallo and A. Neto, "A connected array of slots supporting broadband leaky waves," *IEEE Trans. Antennas Propag.*, vol. 61, no. 4, pp. 1986-1994, 2013.

[20] A. Neto, N. Llombart, J. Baselmans, A. Baryshev, and S. J. C. Yates, "Demonstration of the leaky lens antenna at sub-millimeter wavelengths," *IEEE Trans. Terahertz Sci. Technol.*, vol. 4, no. 1, pp. 26-32, 2014.

[21] Y. Wang, A. S. Helmy, and G. V. Eleftheriades, "Ultra-optical leaky-wave slot antennas," *Opt. Exp.*, vol. 19, no. 13, pp.12392-12401, 2011.

[22] F. Tokan, "Optimization-based matching layer design for broadband dielectric lens antennas," *Applied Computational Electromagnetics Society Journal*, vol. 29, no. 6, pp. 499-507, 2014.

[23] CST Microwave Studio, CST GmbH, 2016. http://www.cst.com

[24] L. Luan, P. R. Sievert, and J. B. Ketterson, "Near-field and far-field electric dipole radiation in the vicinity of a planar dielectric half space," *New Journal of Physics*, vol. 8, pp. 1-11, 2006.

[25] O. Yurduseven, N. L. Juan, and A. Neto, "A dual-polarized leaky lens antenna for wideband focal plane arrays," *IEEE Trans. Antenn. Propag.*, vol. 64, no. 8, pp. 3330-3337, 2016.

Truong Khang Nguyen received the B.S. degree in Computational Physics from the University of Science, Vietnam National University, Ho Chi Minh City in 2006, and the M.S. and Ph.D. degrees in Electrical and Computer Engineering from Ajou University in Suwon, Korea in 2013. From Oct. 2013 to Dec. 2014, he worked at Division of Energy Systems Research, Ajou Univerisity, Korea as a Postdoctoral Fellow. He is currently Head of Division of Computational Physics at Institute for Computational Science, Ton Duc Thang University in Ho Chi Minh City, Vietnam. His current research interests include the design and analysis of microwave, millimeter-wave, terahertz wave, and nano-structured antennas.

Huy Hung Tran received the B.S. degree in Electronics and Telecommunications from Hanoi University of Science and Technology, Hanoi, Vietnam in 2013, and the M.S. degree in the Department of Electrical and Computer Engineering, Ajou University, Suwon, Korea in 2015. His research is focused on wideband circularly polarized, and metamaterial for next generation wireless communication systems.